Molecular Pharmacology Fast Forward. Published on November 1, 2011 as doi:10.1124/mol.111.074252
This article has not been copyedited and formatted. The final version may differ from this version.



# Title

Evidence for a common pharmacological interaction site on $K_{Ca}2$ channels providing both selective activation and selective inhibition of the human $K_{Ca}2.1$ subtype

Charlotte Hougaard, Sofia Hammami, Birgitte L. Eriksen, Ulrik S. Sørensen, Marianne L. Jensen, Dorte Strøbæk, Palle Christophersen.

*NeuroSearch A/S, Pederstrupvej 93, DK-2750 Ballerup, Denmark*

Molecular Pharmacology Fast Forward. Published on November 1, 2011 as DOI: 10.1124/mol.111.074252
This article has not been copyedited and formatted. The final version may differ from this version.



**Running title:**

Positive and negative gating modulation of $K_{Ca}2.1$

**Address correspondence to:**

Palle Christophersen; NeuroSearch A/S, Pederstrupvej 93, DK-2750 Ballerup, Denmark; Tel: +45 44 60 82 22; Fax: +45 44 60 80 80; e-mail: pc@neurosearch.com



**Text pages:**

**Number of tables: 1**

**Number of figures: 8**

**Number of references: 35**

**Words in Abstract: 248**

**Words in Introduction: 745**

**Words in Discussion: 1208**

**Abbreviations:**

B-TPMF, *N*-{7-[1-(4-*tert*-butyl-phenoxy)ethyl]-[1,2,4]triazolo[1,5-*a*]pyrimidin-2-yl}-*N*'-methoxy-formamidine; CaM, calmodulin; CaMBD, calmodulin binding domain; CM-TPMF, *N*-{7-[1-(4-chloro-2-methylphenoxy)ethyl]-[1,2,4]triazolo[1,5-*a*]pyrimidin-2-yl}-*N*'-methoxy-formamidine; CyPPA, cyclohexyl-[2-(3,5-dimethyl-pyrazol-1-yl)-6-methylpyrimidin-4-yl]-amine; DCEBIO, 5,6-dichloro-1-ethyl-1,3-dihydro-2*H*-benzimidazol-2-one; 1-EBIO, 1-ethyl-2-benzimidazolinone; GW542573X, 4-(2-methoxyphenylcarbamoyloxymethyl)-piperidine-1-carboxylic acid *tert*-butyl ester; HEK293, human embryonic kidney 293; $K_{Ca}2$, small

Molecular Pharmacology Fast Forward. Published on November 1, 2011 as DOI: 10.1124/mol.111.074252
This article has not been copyedited and formatted. The final version may differ from this version.



conductance $Ca^{2+}$-activated $K^+$ channel (SK channel); $K_{Ca}3.1$, intermediate conductance $Ca^{2+}$-activated $K^+$ channel (IK channel); NS309, 6,7-dichloro-1*H*-indole-2,3-dione 3-oxime; NS4591, 4,5-dichloro-1,3-diethyl-2,3-dihydro-1*H*-1,3-benzodiazol-2-one; NS8593, (*R*)-*N*-(benzimidazol-2-yl)-tetrahydro-1-naphtylamine; S, transmembrane segment; SKA-31, naphtho[1,2-*d*]thiazol-2-ylamine.

Molecular Pharmacology Fast Forward. Published on November 1, 2011 as DOI: 10.1124/mol.111.074252
This article has not been copyedited and formatted. The final version may differ from this version.



**ABSTRACT**

We have previously identified Ser293 in transmembrane segment 5 as a determinant for selective $K_{Ca}2.1$ channel activation by GW542573X (4-(2-methoxyphenylcarbamoyloxymethyl)-piperidine-1-carboxylic acid *tert*-butyl ester). Now we show that Ser293 mediates both activation and inhibition of $K_{Ca}2.1$: CM-TPMF (*N*-{7-[1-(4-chloro-2-methylphenoxy)ethyl]-[1,2,4]triazolo[1,5-*a*]pyrimidin-2-yl}-*N*'-methoxy-formamidine) and B-TPMF (*N*-{7-[1-(4-*tert*-butyl-phenoxy)ethyl]-[1,2,4]triazolo[1,5-*a*]pyrimidin-2-yl}-*N*'-methoxy-formamidine), two newly identified and structurally related [1,2,4]triazolo[1,5-*a*]pyrimidines, act either as an activator or as an inhibitor of the human $K_{Ca}2.1$ channel. While (-)-CM-TPMF activates $K_{Ca}2.1$ with an $EC_{50}$ value of 24 nM, (-)-B-TPMF inhibits the channel with an $IC_{50}$ value of 31 nM. In contrast, their (+)-enantiomers are 40-100 times less active. Both (-)-CM-TPMF and (-)-B-TPMF are subtype-selective with 10-20 fold discrimination towards other $K_{Ca}2$ channels and the $K_{Ca}3$ channel. Co-application experiments reveal competitive-like functional interactions between the effects of (-)-CM-TPMF and (-)-B-TPMF. Despite belonging to a different chemical class than GW542573X the $K_{Ca}2.1$ selectivity of (-)-CM-TPMF and (-)-B-TPMF depend critically on Ser293 as revealed by loss- and gain-of-function mutations. We conclude that compounds occupying the TPMF site may either positively or negatively influence the gating process depending on their substitution pattern. Notably, (-)-CM-TPMF is 10 times more potent on $K_{Ca}2.1$ than NS309 (6,7-dichloro-1*H*-indole-2,3-dione 3-oxime), an unselective but hitherto the most potent $K_{Ca}3/K_{Ca}2$ channel activator. (-)-B-TPMF is the first small molecule inhibitor with significant selectivity among the $K_{Ca}2$ channel subtypes, and in contrast to peptide blockers like apamin and scyllatoxin, which preferentially affect $K_{Ca}2.2$, (-)-B-TPMF exhibits $K_{Ca}2.1$

Molecular Pharmacology Fast Forward. Published on November 1, 2011 as DOI: 10.1124/mol.111.074252
This article has not been copyedited and formatted. The final version may differ from this version.



selectivity. These high-affinity compounds, which exert opposite effects on $K_{Ca}2.1$ gating, may help define physiological or pathophysiological roles of this channel.

Molecular Pharmacology Fast Forward. Published on November 1, 2011 as DOI: 10.1124/mol.111.074252
This article has not been copyedited and formatted. The final version may differ from this version.



## Introduction

Small and intermediate conductance $Ca^{2+}$-activated $K^+$ channels (the KCNN family: $K_{Ca}2.1$, $K_{Ca}2.2$, $K_{Ca}2.3$, and $K_{Ca}3.1$) contain six transmembrane segments (S1-6) arranged as a tetramer around a central pore. Each subunit associates with one calmodulin (CaM) molecule, acting as a β-subunit at the C-terminal CaM binding domain (CaMBD) (Xia et al., 1998; Khanna et al., 1999). $Ca^{2+}$ binding to CaM rearranges the CaM/CaMBD region and the S6/S5 domains, thereby opening the channel. The nature of the gate remains elusive but cysteine scanning experiments have narrowed down its possible location to residues in the inner pore vestibule close to the selectivity filter. In contrast to $K_v$ channels, KCNN channels are assumed to exhibit "deep pore gating" (Bruening-Wright et al., 2007; Bruening-Wright et al., 2002; Garneau et al., 2009; Klein et al., 2007), which is important for the understanding of the molecular pharmacology of positive and negative KCNN channel gating modifiers.

The $K_{Ca}2$ channel subtypes are widely and distinctly expressed in the CNS, controlling somatic excitability, pacemaker firing rates, and synaptic plasticity (Pedarzani and Stocker, 2008; Bond et al, 2005). Clinically used drugs with $K_{Ca}2$ activating properties are the centrally acting muscle relaxants zoxazolamine and chlorzoxazone, which are used for treating spasticity, and riluzole, which is registered for amyotropic lateral sclerosis. The $K_{Ca}2$-facilitating properties (probably $K_{Ca}2.2$) of both chlorzoxazone and riluzole have recently been suggested to account for their beneficial effects in rodent ataxia models (Alviña and Khodakhah, 2010; Janahmadi et al., 2009) and in patients (Ristori et al., 2010). Arguably, $K_{Ca}2$ activation (probably $K_{Ca}2.3$) also underlies reduced craving and dampening of excessive alcohol intake observed with chlorzoxazone in rats (Hopf et al., 2011). Important hallmarks for a therapeutic $K_{Ca}2$-facilitating mechanism of these drugs are that 1-EBIO (1-ethyl-2-benzimidazolinone), the prototype KCNN channel activator,

Molecular Pharmacology Fast Forward. Published on November 1, 2011 as DOI: 10.1124/mol.111.074252
This article has not been copyedited and formatted. The final version may differ from this version.



exerts a similar anti-ataxic action when applied locally into the cerebellum of tottering mice (Walter et al., 2006) and anti-addictive effect against alcohol when applied into rat nucleus accumbens core region (Hopf et al., 2010). In contrast, inhibition of $K_{Ca}2$ channels has not been demonstrated to account for clinical efficacy of any drug. The anti-depressant fluoxetine is a weak blocker of cloned $K_{Ca}$ channels (Terstappen et al., 2003) and $K_{Ca}2.3$ channel block may mediate an anti-depressant mechanism (Galeotti et al., 1999, Jacobsen et al., 2008). However, it is doubtful whether this mechanism for fluoxetine plays a role compared to serotonin transporter inhibition.

Validation of specific $K_{Ca}$ channel subtypes as targets for CNS drug discovery is hampered by lack of selective and potent molecules that pass the blood brain barrier. Classic $K_{Ca}2$ channel blockers like UCL1684 (6,10-diaza-3(1,3),8(1,4)-dibenzena-1,5(1,4)-diquinolinacyclodecaphane) mimic the inhibition by the $K_{Ca}2$ selective peptide apamin, and are unselective among the $K_{Ca}2$ subtypes. Like apamin, they further contain basic and charged moieties that limit their passage into the CNS. 1-EBIO and the $K_{Ca}2$-activating drugs are non-selective $K_{Ca}2$ enhancers and act more potently on $K_{Ca}3.1$. Unfortunately this is also the case for the more potent positive modulators DCEBIO, NS309, NS4591 and SKA-31, even though these have emerged from dedicated chemical optimization programs (Wulff and Zhorov, 2008).

Subtype-selective positive gating modulators and non-selective negative gating modulators have recently been identified. These have been instrumental in defining new sites and new modes-of-actions for gating modulation of $K_{Ca}2$ channels. The negative gating modulator NS8593 ((*R*)-*N*-(benzimidazol-2-yl)-tetrahydro-1-naphtylamine), causes a reduction in the apparent $Ca^{2+}$-sensitivity for channel activation (Strøbæk et al., 2006, Sørensen et al., 2008). This effect depends on Ser507 and Ala532 ($K_{Ca}2.3$ numeration) positioned in the S5 pore helix and S6

Molecular Pharmacology Fast Forward. Published on November 1, 2011 as DOI: 10.1124/mol.111.074252
This article has not been copyedited and formatted. The final version may differ from this version.



transmembrane segment just below the selectivity filter and was therefore interpreted as NS8593-interaction with deep pore gating structures (Jenkins et al., 2011). These amino acids are conserved among the $K_{Ca}2$ channels, thus explaining the lack of $K_{Ca}2$ subtype selectivity of NS8593 and close analogues (Sørensen et al., 2008). The $K_{Ca}2.1$ selective activator GW542573X, which acts dually by directly opening the channel and by increasing the apparent $Ca^{2+}$-sensitivity (Hougaard et al., 2009), depends on Ser293 in the S5 transmembrane helix, a $K_{Ca}2.1$ specific amino acid. These mixed effects differ significantly from the mode-of-action of non-selective activators, but also from the $K_{Ca}2.2/3$ selective modulator CyPPA (cyclohexyl-[2-(3,5-dimethyl-pyrazol-1-yl)-6-methylpyrimidin-4-yl]-amine), which increases the apparent $Ca^{2+}$-sensitivity via interaction with the C-terminal (Hougaard et al., 2007; Li et al., 2009; Pedarzani et al., 2001).

Here we describe two novel and closely related [1,2,4]triazolo[1,5-*a*]pyrimidines, (-)-CM-TPMF and (-)-B-TPMF, which both exhibit high-potency (~30 nM) and subtype-selective interactions with $K_{Ca}2.1$ via Ser293. These compounds show opposite functions with (-)-CM-TPMF acting as an activator and (-)-B-TPMF as an inhibitor.

Molecular Pharmacology Fast Forward. Published on November 1, 2011 as DOI: 10.1124/mol.111.074252
This article has not been copyedited and formatted. The final version may differ from this version.



## Materials and Methods

*Chemistry*

B-TPMF ((*N*-{7-[1-(4-*tert*-butyl-phenoxy)ethyl]-[1,2,4]triazolo[1,5-*a*]pyrimidin-2-yl}-*N*'-methoxy-formamidine) and CM-TPMF (*N*-{7-[1-(4-chloro-2-methylphenoxy)ethyl]-[1,2,4]triazolo[1,5-*a*]pyrimidin-2-yl}-*N*'-methoxy-formamidine) were purchased as racemates from Key Organics Ltd, Camelford, Cornwall, UK. The compounds were resolved into their enantiomeric pairs by preparative chiral chromatography using for B-TPMF a Chiracel OD-H column (solvent 40% ethanol in hexane, flow rate 1.0 ml/min) and for CM-TPMF a Chiralpak AD-H column (solvent 40% ethanol in hexane, flow rate 1.0 ml/min). Determination of chiral purity was performed on an analytical Waters Thar Investigator instrument equipped with a PDA detector: for B-TPMF using a Phenomenex Lux2 column, 250 x 4.6 mm, 5 µm particle size (solvent super critical $CO_2$ with ethanol as co-solvent and isocratic elution with 45% co-solvent and a flow rate of 3.2 ml/min); for CM-TPMF using a Phenomenex Lux1 Column, 250 x 4.6 mm, 5 µm particle size (solvent super critical $CO_2$ with methanol as co-solvent and isocratic elution with 40% co-solvent and a flow rate of 3.2 ml/min). Chiral purity was determined by integration of the PDA (total absorbance) trace. Optical rotations were measured on a Perkin Elmer polarimeter (model 314). Absolute configurations were not determined. NMR spectra were recorded on a Bruker ultra shield plus 400 MHz (Advance II) instrument. Characterization of (-)-B-TPMF ($C_{19}H_{24}N_6O_2$): Specific optical rotation $[\alpha]_D^{25}$= -291° ($CHCl_3$); enantiomeric excess (ee) >99%; HR-MS(ES+) m/z 369.20362 ([M + 1]+, 100%), calcd. 369.20328; $^1$H NMR ($CDCl_3$) δ 1.26 (s, 9H), 1.78 (d, 3H, *J* = 6.6 Hz), 3.92 (s, 3H), 5.89 (q, 1H, *J* = 6.5 Hz), 6.75 (m, 2H) , 7.10 (m, 2H), 7.25 (m, 2H), 7.82 (d, 1H, *J* = 10.4 Hz), 7.98 (d, 1H, *J* = 10.4 Hz); 8.60 (d, 1H *J* = 4.7 Hz). Characterization of (-)-CM-TPMF ($C_{16}H_{17}ClN_6O_2$): Specific optical

Molecular Pharmacology Fast Forward. Published on November 1, 2011 as DOI: 10.1124/mol.111.074252
This article has not been copyedited and formatted. The final version may differ from this version.



rotation $[\alpha]_D^{25}$ = -275° ($CHCl_3$); ee = 96.4%; HR-MS(ES+) m/z 361.11775 ([M + 1]+, 100%), calcd. 361.11738; $^1$H NMR ($CDCl_3$) δ 1.80 (d, 3H, *J* = 6.5 Hz), 2.34 (s, 3H), 3.93 (s, 3H), 5.89 (q, 1H, *J* = 6.4 Hz), 6.44 (d, 1H, *J* = 8.8 Hz), 6.95-7.04 (m, 2H), 7.17 (m, 1H), 7.81(d, 1H, *J* = 10.4 Hz), 7.97 (d, 1H, *J* = 10.2), 8.61 (d, 1H, *J* = 4.7 Hz).

*Molecular biology.*

The generation of point mutated $hK_{Ca}2.3_{L476S}$ has been described previously (Hougaard et al., 2009) and $hK_{Ca}2.1_{S293L}$ was generated by mutagenesis on $hK_{Ca}2.1$. Briefly, the plasmid encoding $hK_{Ca}2.1$ was uracilated by the *E. Coli* RZ1032 and used as template in a mutagenesis reaction utilizing the oligonucleotide GTGCTGCTGGTCTTCtcgATaTCCctCTGGATCATCGCAGC, T7 DNA polymerase and T4 DNA ligase. The mutation was verified by sequencing.

*Cell cultures*

For patch clamp experiments with $hK_{Ca}2.1$, $hK_{Ca}2.2$, $hK_{Ca}2.3$ and $hK_{Ca}3.1$, HEK293 cell lines stably expressing these channels were used (Hougaard et al., 2009). Point mutated channels ($hK_{Ca}2.1_{S293L}$ and $hK_{Ca}2.3_{L476S}$) were transiently transfected into HEK293 cells using Lipofectamine (Invitrogen, Carlsbad, CA) and standard transfection methods. Electrophysiological measurements were performed 2-3 days after transfection. Cells were cultured in Dulbecco's Modified Eagle's Medium (DMEM, Sigma-Aldrich, Brøndby, Denmark) enriched with 10% fetal calf serum (FCS, Gibco, Invitrogen, NY, USA) at 37°C and 5% $CO_2$. At approximately 75% confluence, the cells were washed once with phosphate buffered saline (PBS), harvested by trypsin/EDTA (Sigma-Aldrich) treatment and transferred to petri dishes containing cover slips (∅ 3.5 mm, purchased from VWR international, Herlev, Denmark).

Molecular Pharmacology Fast Forward. Published on November 1, 2011 as DOI: 10.1124/mol.111.074252
This article has not been copyedited and formatted. The final version may differ from this version.



*Electrophysiology*

Membrane currents were recorded using the whole-cell or the inside-out configuration of the patch-clamp technique. Cells seeded on cover slips were transferred to a 15 µl recording chamber and continuously superfused at 1 ml $min^{-1}$. An integrated Ag/AgCl pellet electrode served as reference. Experiments were conducted at room temperature. Patch pipettes (approx. 2 MΩ) were pulled from borosilicate tubes with an outside diameter of 1.32 mm (Vitrex Medical, Herlev, Denmark) using a horizontal electrode puller (Zeitz Instruments, Augsburg, Germany). An electronically controlled micromanipulator (Eppendorf, Radiometer, Denmark) was used for the positioning of pipettes and the experiments were controlled by an EPC-9 amplifier (HEKA, Lambrecht, Germany). Data were filtered at 3 kHz. Currents were elicited by applying a 200 ms linear voltage ramp from -80 to +80 mV every 5 s from a holding potential of 0 mV. In whole-cell experiments, the cell capacitance and series resistance ($R_s$ below 8 MΩ, 80% compensation) were updated before each voltage ramp.

In all experiments a solution with a high $K^+$ concentration was applied to the extracellular side of the membrane (in mM): 154 KCl, 2 $CaCl_2$, 1 $MgCl_2$ and 10 HEPES, pH adjusted to 7.4 with 1 M KOH. The intracellular solutions contained (in mM): 154 KCl, 10 HEPES, 10 EGTA, or a combination of EGTA and NTA (10 mM in total). Concentrations of $MgCl_2$ and $CaCl_2$ required to obtain the desired free concentrations ($Mg^{2+}$ always 1 mM, $Ca^{2+}$ 0.01 – 10 µM) were calculated (EqCal, Cambridge, UK) and added. In the nominal $Ca^{2+}$-free intracellular solution, no $Ca^{2+}$ was added. The intracellular solutions were adjusted to pH 7.2 with 1 M KOH.

Molecular Pharmacology Fast Forward. Published on November 1, 2011 as DOI: 10.1124/mol.111.074252
This article has not been copyedited and formatted. The final version may differ from this version.



*Calculations and statistics*

In inside-out experiments $EC_{50}$ and $IC_{50}$ as well as $n_{Hill}$ values for compounds and $Ca^{2+}$ were estimated from equilibrium concentration-response relationships by fitting to the Hill-equation. In whole-cell experiments, $EC_{50}$ values for current activation are not readily determined due to poor clamping conditions at higher degrees of channel activation. Instead the concentrations of compound giving 100 % current increase (called the $SC_{100}$ value, see Table 1) were estimated. In some experiments $K_d$ values were calculated from single concentration applications by fitting to the kinetics of inhibition (see Strøbæk et al., 2006).

All results are presented as the mean ± standard error of the mean (S.E.M.) with the number of experiments indicated. Significance testing was performed by Student´s t-test for unpaired samples.

Molecular Pharmacology Fast Forward. Published on November 1, 2011 as DOI: 10.1124/mol.111.074252
This article has not been copyedited and formatted. The final version may differ from this version.



**Results**

The chemical structures of the two new compounds B-TPMF (*N*-{7-[1-(4-*tert*-butyl-phenoxy)ethyl]-[1,2,4]triazolo[1,5-*a*]pyrimidin-2-yl}-*N*'-methoxy-formamidine) and CM-TPMF (*N*-{7-[1-(4-chloro-2-methylphenoxy)ethyl]-[1,2,4]triazolo[1,5-*a*]pyrimidin-2-yl}-*N*'-methoxy-formamidine) as well as GW542573X are shown in Fig. 1. The effects of the isolated enantiomers of B-TPMF and CM-TPMF (Materials and Methods, chemistry section) were determined in whole-cell voltage-clamp experiments by applying 10 nM of the compounds to HEK293 cells expressing human $K_{Ca}2.1$ channels. Representative current traces are shown in Fig. 2A and the current recorded at -75 mV is plotted vs. time in Fig. 2B. The (-)-enantiomer of B-TPMF *inhibited* the $K_{Ca}2.1$ current, whereas the (+)-enantiomer was without effect. In contrast, (-)-CM-TPMF, induced a robust *activation,* again with the (+)-enantiomer exerting no effect. The time course of this experiment (Fig. 2B) underscores the reversibility of these actions and the I-V curves show preservation of the normal inward rectification in presence of all compounds. Fig. 2C summarizes this series of experiments and specifically documents that 10 nM of (-)-B-TPMF significantly ($p < 0.001$, students t-test for unpaired samples) inhibits the $K_{Ca}2.1$ current, while (-)-CM-TPMF enhances it. The corresponding (+)-enantiomers of both compounds in contrast are inactive at this concentration. Whole-cell experiments were also performed in order to quantify the enantiomer selectivity (experiments not illustrated): $K_d$ values for (+)-B-TPMF and (-)-B-TPMF were 1.6 ± 0.5 µM (n = 5) and 15 ± 7 nM (n = 5), respectively. Similarly, (+)-CM-TPMF activated $K_{Ca}2.1$ with an $SC_{100}$ of 200 ± 44 nM (n = 5) compared to 5 ± 0.2 nM (n = 6) for (-)-CM-TPMF. Thus, for B-TPMF and CM-TPMF the activity on $K_{Ca}2.1$ channels primarily resides in the (-) enantiomers with enantiomer selectivities of ~100 fold and ~40 fold.

Molecular Pharmacology Fast Forward. Published on November 1, 2011 as DOI: 10.1124/mol.111.074252
This article has not been copyedited and formatted. The final version may differ from this version.



To investigate the subtype selectivity of the more active (-)-enantiomers experiments were conducted on HEK293 cells stably expressing $hK_{Ca}2.1$, $hK_{Ca}2.2$ or $hK_{Ca}2.3$ channels (Fig. 3). Since (-)-B-TPMF and (-)-CM-TPMF act equally well from both sides of the membrane, the inside-out configuration of the patch-clamp technique was chosen in order to achieve a well defined $[Ca^{2+}]_i$. At a concentration of 30 nM, (-)-B-TPMF inhibited the $K_{Ca}2.1$ current by approximately 50% whereas conversely (-)-CM-TPMF induced a 3-fold increase. At the same concentration only minor effects were detectable on $K_{Ca}2.2$ and $K_{Ca}2.3$ (Fig. 3A) indicating that both compounds exhibit selectivity for $K_{Ca}2.1$ over the closely related isoforms. Full concentration-response relationships were obtained for the three $K_{Ca}2$ subtypes and results for both compounds are summarized in Fig. 3B and 3C. The data generated for (-)-B-TPMF-induced inhibition conformed well to the Hill-equation with an $IC_{50}$ value for $K_{Ca}2.1$ of approximately 30 nM and a complete inhibition of the current at 1 µM, whereas $K_{Ca}2.2$ and $K_{Ca}2.3$ both were inhibited with $IC_{50}$ values around 1 µM (see Table 1, and text to Fig. 3). Hence (-)-B-TPMF is a selective inhibitor of $K_{Ca}2.1$ which displays approximately 30-fold selectivity over the other $K_{Ca}2$ channels. The concentration-response relationships obtained from applications of (-)-CM-TPMF to marginally activated $K_{Ca}2$ channels (0.2 µM $Ca^{2+}$, degree of activation ~ 15%) yielded an $EC_{50}$ value of 24 nM for $K_{Ca}2.1$ and a maximal degree of activation of approximately 80 % compared to a $[Ca^{2+}]_i$ of 10 µM. $K_{Ca}2.2$ and $K_{Ca}2.3$ were activated with $EC_{50}$ values of 290 and 250 nM showing that (-)-CM-TPMF is 10-fold more selective for $K_{Ca}2.1$. Similar selectivity ratios were obtained against $K_{Ca}3.1$except for (-)-CM-TPMF, which acted as a (very weak) activator (Table 1). Table 1 also summarizes the effects of (-)-CM-TPMF and (-)-B-TPMF on more distantly related ion channels. Only marginal inhibitory effects were observed for both compounds at 10 µM on members of other $K^+$ channel gene families ($K_{Ca}1.1$, $K_v7.2$+$K_v7.3$,

Molecular Pharmacology Fast Forward. Published on November 1, 2011 as DOI: 10.1124/mol.111.074252
This article has not been copyedited and formatted. The final version may differ from this version.



and $K_v11.1$) as well as $Na_v1.2$ channels. A broader selectivity profile was obtained for the two racemates by testing at concentrations of 10 µM in the 69 receptor LeadProfilerScreen (PT# 1107076) at MDSPharma (now Ricerca Biosciences LLC), Taiwan. Neither of the racemates reached the pre-defined significance criteria of > 50 % effect in any assay.

We next investigated the mode-of-actions of (-)-CM-TPMF and (-)-B-TPMF. Classic enhancers of $K_{Ca}2$ channel activity increase the apparent $Ca^{2+}$-sensitivity and are unable to activate the channels in the absence of intracellular $Ca^{2+}$. In contrast, GW542573X (see Fig. 1), a recently described $K_{Ca}2.1$ selective compound, acts by a dual mechanism, increasing the apparent $Ca^{2+}$-sensitivity and inducing a small $Ca^{2+}$-independent channel activation. Fig. 4A shows the time course of an inside-out experiment where the $[Ca^{2+}]_i$ was varied (0, 0.2, and 10 µM) and the ability of 100 nM (-)-CM-TPMF to activate the $K_{Ca}2.1$ current at each $Ca^{2+}$ concentration was investigated. Fig. 4B shows the corresponding I-V relationships. Addition of (-)-CM-TPMF clearly enhanced the $K_{Ca}2.1$ current in the nominal absence of $Ca^{2+}$ and shifted the I-V relationship from a small, non-specific linear leak current to an inwardly rectifying current typical for $K_{Ca}2$ channels recorded under symmetrical $K^+$ conditions. At an intermediate $Ca^{2+}$ concentration of 200 nM, where the $K_{Ca}2.1$ channels are partially $Ca^{2+}$-activated, as well as at saturating $Ca^{2+}$ concentrations of 10 µM, where the channels are maximally activated, application of (-)-CM-TPMF induced an increase in the current level. At all $[Ca^{2+}]_i$ the current measured in the presence of (-)-CM-TPMF maintained the characteristic inward rectification. Fig. 4C shows the $Ca^{2+}$-response relationship of $K_{Ca}2.1$ in the absence of compound (Ctrl) as well as in the presence of 0.1 µM or 1 µM of (-)-CM-TPMF. Notably, (-)-CM-TPMF exerts a dual action on the $K_{Ca}2.1$ channel, consisting of a leftward shift in the $Ca^{2+}$-response curve (i.e. positive modulation) as well as a substantial direct activating effect, which is independent of

Molecular Pharmacology Fast Forward. Published on November 1, 2011 as DOI: 10.1124/mol.111.074252
This article has not been copyedited and formatted. The final version may differ from this version.



$Ca^{2+}$ (close to 40% at low $Ca^{2+}$ and in the presence of 1 μM of (-)-CM-TPMF). Thus, from a mode-of-action perspective, (-)-CM-TPMF belongs to the GW542573X functional class of $K_{Ca}2.1$ activators. Quantitatively, however, (-)-CM-TPMF is considerably more potent (> 100 fold) than GW542573X and the fraction of $Ca^{2+}$-independent activation induced by the compound is much larger (~40 % vs. 5 %).

$K_{Ca}2$ channels are inhibited by peptides like apamin and scyllatoxin as well as small molecules carrying positive charges mimicking the charges on apamin. These molecules bind from the outside, and despite an allosteric of apamin (Lamy et al., 2010), their inhibition is independent of the degree of channel activation by $Ca^{2+}$. In contrast, negative gating modulators like NS8593 interfere with the gating mechanism of $K_{Ca}2$ channels, causing reduced apparent affinity for $Ca^{2+}$. A characteristic feature of this mode-of-action is potent inhibition at low $[Ca^{2+}]_i$ and reduced effect at higher $Ca^{2+}$ concentrations. The following experiment was designed in order to elucidate whether the inhibition by (-)-B-TPMF is dependent on the $[Ca^{2+}]_i$. Fig. 5A shows the time course of an inside-out experiment were the ability of 30 nM of (-)-B-TPMF to inhibit the $K_{Ca}2.1$ was evaluated at two different $Ca^{2+}$ concentrations: 0.3 μM - equal to approximately 30% of maximal channel activity - and 10 μM $Ca^{2+}$ corresponding to maximal activity. (-)-B-TPMF inhibited approximately 75 % of the current at the lower $Ca^{2+}$ concentration, whereas it only inhibited about 20 % at 10 μM $Ca^{2+}$. In Fig. 5B the degree of inhibition by 30 nM (-)-B-TPMF at three $Ca^{2+}$ concentrations (0.3-, 0.5-, and 10 μM) is quantified. The effect is clearly dependent on the intracellular $Ca^{2+}$ concentration/channel activity and (-)-B-TPMF accordingly fulfills the criteria for being a negative gating modulator.

Due to the very similar structures of (-)-B-TPMF and (-)-CM-TPMF we envisioned that they might interact with a common binding site on $K_{Ca}2.1$. To test this hypothesis we conducted a

Molecular Pharmacology Fast Forward. Published on November 1, 2011 as DOI: 10.1124/mol.111.074252
This article has not been copyedited and formatted. The final version may differ from this version.



series of patch clamp experiments in order to elucidate possible competitive-like functional interactions. In the first series of experiments we investigated whether $K_{Ca}2.1$ activated by different concentrations (1 and 10 μM) of (-)-CM-TPMF would affect experimentally determined $IC_{50}$ values for (-)-B-TPMF. These concentrations of (-)-CM-TPMF were chosen as they both induce near maximal activation of $K_{Ca}2.1$ (see Fig. 3C) at a permissive fixed $[Ca^{2+}]_i$ of 200 nM. Fig. 6A shows the I-V relations obtained in the presence of 1μM (left panel) and 10 μM (right panel) of (-)-CM-TPMF. When 1 μM (-)-B-TPMF was co-applied, an approximate 60% reduction in the current activated by 1μM (-)-CM-TPMF was obtained, whereas the same concentration of (-)-B-TPMF only inhibited 15% of the current activated by 10 μM (-)-CM-TPMF. Inhibition curves for (-)-B-TPMF were generated and Fig. 6B clearly shows that increasing the concentration of (-)-CM-TPMF from 1 to 10 μM resulted in an increase in the $IC_{50}$-value of (-)-B-TPMF from 0.43 μM to 2.96 μM. Although no rigorous comparison is possible it is noteworthy that the $IC_{50}$ value for (-)-B-TPMF at 200 nM $[Ca^{2+}]_i$ in the absence of (-)-CM-TPMF is expected to be in the low nM range (Fig. 5). In the second series of experiments we attempted to prove that the increase in $IC_{50}$ values in the presence of (-)-CM-TPMF is dependent of the presence of this compound *per se*, rather than being an effect of the high open state probability prevailing under the experimental conditions in Fig. 6. Therefore, we compared the inhibition by (-)-B-TPMF at high $[Ca^{2+}]_i$ (10 μM) with the inhibition at semi-maximal $[Ca^{2+}]_i$ (0.5 μM) in combination with 3 μM (-)-CM-TPMF resulting in similar degrees of activation (Fig. 7). The time-course of the experiment (Fig. 7A) shows that at 10 μM $Ca^{2+}$, (-)-B-TPMF (0.1 μM) inhibits the current reversibly by 75%. However, after wash-out and reactivation with 0.5 μM $Ca^{2+}$ + 3 μM (-)-CM-TPMF, no effect was observed of 0.1 μM (-)-B-TPMF, and even a 100 times higher concentration was needed in order to get the same degree of inhibition as when

Molecular Pharmacology Fast Forward. Published on November 1, 2011 as DOI: 10.1124/mol.111.074252
This article has not been copyedited and formatted. The final version may differ from this version.



the channel was similarly activated by $Ca^{2+}$ alone. Note also the strongly reduced rate of inhibition compared to the faster rate obtained at 0.1 µM (-)-B-TPMF at the first addition. We conclude from these experiments that (-)-B-TPMF and (-)-CM-TPMF interact functionally on the $K_{Ca}2.1$ channel in a manner likely to reflect direct competition on a common binding site.

The action of both positive and negative modulators of $K_{Ca}2$ channels depend on very specific amino acid residues. 1-EBIO and CyPPA interact with the intracellular C-terminal CaMBD, whereas NS8593 depends on transmembrane amino acids. The $K_{Ca}2.1$-selective activator GW542573X acts via a single amino acid, Ser293, located in the S5 transmembrane region of $K_{Ca}2.1$. Due to the similar mode-of-action of GW542573X and (-)-CM-TPMF we conducted a series of experiments in order to investigate the possible involvement of Ser293 in the actions of both (-)-CM-TPMF and (-)-B-TPMF. Two point-mutated $K_{Ca}2$ channels were used, one ($K_{Ca}2.1_{S293L}$) in which Ser293 in $K_{Ca}2.1$ is substituted with the equivalent leucine (Leu321 in $K_{Ca}2.2$ and Leu476 in $K_{Ca}2.3$) and one with the reverse mutation (Leu476 in $K_{Ca}2.3$ changed to serine, $K_{Ca}2.3_{L476S}$; see Fig. 8A for approximate position in S5 and amino acid alignment of the S5 region of $K_{Ca}2.1$ and $K_{Ca}2.3$). Both channel constructs were activated by $[Ca^{2+}]_i$ within the normal range with $EC_{50}$ values of 0.44 ± 0.05 µM ($K_{Ca}2.1_{S293L}$, n = 3) and 0.47 ± 0.06 µM ($K_{Ca}2.3_{L476S}$, n = 4). At 30 nM, a compound concentration that significantly modulated $K_{Ca}2.1$ but had limited effect on $K_{Ca}2.3$ (see Fig. 3), both (-)-CM-TPMF and (-)-B-TPMF failed to affect $K_{Ca}2.1_{S293L}$ (Fig. 8B) but, on the other hand, significantly modulated the $K_{Ca}2.3_{L476S}$ current level (Fig 8C). Full concentration-response relationships were generated for (-)-B-TPMF (Fig. 8D) and (-)-CM-TPMF (Fig. 8E) on $K_{Ca}2.1_{S293L}$ and $K_{Ca}2.3_{L476S}$ in excised inside-out patches. For comparison, the best fit curves for $K_{Ca}2.1$ and $K_{Ca}2.3$, obtained from Fig. 3, are included as dotted lines. As seen from the figure, data obtained on $K_{Ca}2.1_{S293L}$ was similar to those generated

Molecular Pharmacology Fast Forward. Published on November 1, 2011 as DOI: 10.1124/mol.111.074252
This article has not been copyedited and formatted. The final version may differ from this version.



on $K_{Ca}2.3$, thus demonstrating full loss-of-sensitivity both with respect to inhibition by (-)-B-TPMF and activation by (-)-CM-TPMF. Likewise, data obtained on $K_{Ca}2.3_{L476S}$ was virtually identical to those on $K_{Ca}2.1$, demonstrating full gain-of-sensitivity of the $K_{Ca}2.3_{L476S}$ construct for both compounds.

Molecular Pharmacology Fast Forward. Published on November 1, 2011 as DOI: 10.1124/mol.111.074252
This article has not been copyedited and formatted. The final version may differ from this version.



## Discussion

We have described two structurally related compounds as new pharmacological modulators of $Ca^{2+}$-activated $K^+$ channels belonging to the KCNN gene family. Both are [1,2,4]triazolo[1,5-*a*]pyrimidines, a chemical series hitherto not described as having ion channel modulating properties. Both (-)-CM-TPMF and (-)-B-TPMF potently modulated the $K_{Ca}2.1$ subtype while having considerably weaker activity on $K_{Ca}2.2$, $K_{Ca}2.3$ and $K_{Ca}3.1$. (-)-CM-TPMF is a mixed opener/positive gating modulator, whereas the analogue (-)-B-TPMF is a negative gating modulator. Co-application experiments clearly revealed competition-like interactions between (-)-CM-TPMF and (-)-B-TPMF and the high-affinity actions of both compounds were shown to depend critically on the Ser293 positioned in the S5 segment as demonstrated by loss-of-sensitivity ($K_{Ca}2.1_{S293L}$) as well as gain-of-sensitivity ($K_{Ca}2.3_{L476S}$) mutations. Structurally, CM-TPMF and B-TPMF are remarkably similar and the pharmacology leading to either positive or negative gating modulation is determined entirely by the substituents on the terminal phenyl ring, a 4-*tert*-butyl group in B-TPMF or 4-chloro-2-methyl substitution in CM-TPMF. We are currently further exploring the structural components leading to either activation or inhibition and the general structure-activity relationship associated with chemical modification within this compound class (Eriksen et al., 2010a, b, and c). Interestingly, for each of these compounds the chirality introduced by the carbon atom in the linker separating the phenyl and the bicyclic heteroaromatic groups, led to pairs consisting of a highly potent (-)-enantiomer and a 40-100 fold less active (+)-isomer. Overall we conclude that $K_{Ca}2$ channels - in particular the $K_{Ca}2.1$ isoform - possess a common high-affinity binding-site for (-)-[1,2,4]triazolo[1,5-*a*]pyrimidines, here exemplified by (-)-CM-TPMF and (-)-B-TPMF, that pivotally influences the gating process in a facilitating or dampening way depending on minor changes in the substitution pattern of the

Molecular Pharmacology Fast Forward. Published on November 1, 2011 as DOI: 10.1124/mol.111.074252
This article has not been copyedited and formatted. The final version may differ from this version.



interacting molecules. This is the first demonstration of a common site for both positive and negative pharmacological modulation of gating in $K_{Ca}$ channels, a phenomenon which is well established for the dihydropyridine pharmacology of L-type $Ca^{2+}$ channels (i.e. nifedipine vs. Bay-k-8644, Greenberg et al., 1984) as well as for the benzodiazepine pharmacology of $GABA_A$ receptors (i.e. diazepam vs. DMCM, Sieghart, 1994).

It is interesting to compare the chemical structures of CM-TPMF/B-TPMF with the previously described (Hougaard et al., 2009) non-chiral and lower-potency $K_{Ca}2.1$ activator GW542573X (Fig. 1), which also depends on Ser293, and which has a qualitatively identical opener/positive modulator mode-of-action as described here for (-)-CM-TPMF. Both structural classes are relatively flexible, small-molecules of similar sizes and molecular weights, both classes contain a terminal phenyl ring, although with different substitution pattern, and both GW542573X and the [1,2,4]triazolo[1,5-*a*]pyrimidines have a single potential hydrogen bond donating group and 7-8 hydrogen bond acceptors. Still, it is evident that GW542573X represents a structurally very different compound class containing two carbamate functionalities of which one contains a terminal *tert*-butyl group also present in B-TPMF. Despite this apparent point of similarity it should be noted that GW542573X is an activator, whereas a closer structure activity analysis comprising further structural analogues (not shown) revealed that the *tert*-butyl group is crucial for the effect of B-TPMF as an inhibitor. Overall, based on the structural differences described above and also the fact that the small structural difference arising from chirality has such detrimental effects on the pharmacology in CM-TPMF and B-TPMF, we consider it unlikely that the [1,2,4]triazolo[1,5-*a*]pyrimidines described herein, would have exactly identical interaction points as GW542573X and share an identical binding site. Despite the parallels between GW542573X and (-)-CM-TPMF in terms of mode-of-action and interaction with Ser293, we

Molecular Pharmacology Fast Forward. Published on November 1, 2011 as DOI: 10.1124/mol.111.074252
This article has not been copyedited and formatted. The final version may differ from this version.



therefore cannot exclude that it actually interacts with a neighbouring site to the [1,2,4]triazolo[1,5-*a*]pyrimidines and just shares the Ser293 and the positive coupling to the gate with (-)-CM-TPMF as down-stream functional effects. From this follows also uncertainty, whether Ser293 *per se* actually constitutes part of the physical binding site for the [1,2,4]triazolo[1,5-*a*]pyrimidines.

Very recently a series of experiments exploring the apparent $Ca^{2+}$ affinity of $rK_{Ca}2.2$ through mutational analysis demonstrated the complexity and the extended distribution of amino acids participating in or influencing the gating process in $rK_{Ca}2.2$ channels (Li and Aldrich, 2011): Charged residues in S6 were found to form a ring of positivity near the inner pore mouth that causes intrinsic rectification, but also influences the gating via an electrostatic mechanism, in particular by keeping the open state probability very low at zero $Ca^{2+}$. Charge reversal mutations of these amino acids strongly increase the open state probability at zero $Ca^{2+}$ and very significantly left-shift the $Ca^{2+}$ activation curve. Without in anyway suggesting a common causality, these findings are phenomenologically very similar to the effects of (-)-CM-TPMF and GW542573X, and serve to illustrate the point that amino acids in the transmembrane segments, far away from the CaM/CaMBD in the C-terminal, are pivotally important for gating and determining apparent $Ca^{2+}$-affinity of $K_{Ca}2$ channels.

The physiological role of the $K_{Ca}2.1$ subtype remains obscure in contrast to the $K_{Ca}2.2$ and $K_{Ca}2.3$ subtypes, which, through their contribution to action potential afterhyperpolarizations and functional coupling with the NMDA receptor, are involved in controlling firing-precision in pacemaking neurons and determining synaptic plasticity (Bond et al., 2005). $K_{Ca}2.1$ is predominantly expressed in the cortical/limbic structures of the brain, a distribution overlapping to a large extent with the expression of $K_{Ca}2.2$, but is essentially absent from the basal ganglia

Molecular Pharmacology Fast Forward. Published on November 1, 2011 as DOI: 10.1124/mol.111.074252
This article has not been copyedited and formatted. The final version may differ from this version.



and monoaminergic neurons, where $K_{Ca}2.3$ is the dominating subtype. Importantly, $K_{Ca}2.1$ is also the KCNN subtype with the most specific CNS expression and appears confined to neurons (Rimini et al., 2000). In contrast, the other KCNN members are also broadly expressed in the periphery on both neurons and somatic cell types and $K_{Ca}2.3$ is also present on glia cells (Armstrong et al., 2005). A serious obstacle towards exploration of the physiology of the $K_{Ca}2.1$ channel is the inability of the rat (and mouse) isoforms to express recombinantly in oocytes as well as mammalian cells. Furthermore, the phenotype of the $K_{Ca}2.1$ knock out mouse is still largely unknown, although it has been reported that the mAHP in CA1 is unaltered in these mice (Bond et al., 2004). An additional complication is the lack of subtype selective tools targeting $K_{Ca}2.1$. In contrast to GW542573X, which is not very potent ($EC_{50}$ ~ 7 µM) both (-)-CM-TPMF and (-)-B-TPMF are high potency $K_{Ca}2.1$ modulators (~30 nM) which display acceptable selectivity over $K_{Ca}2.2$ and $K_{Ca}2.3$ and good to excellent selectivity over other ion channels and receptors. In particular, we envision that the "package" of the two very close analogues with opposite effects on $K_{Ca}2.1$ may constitute a useful combination for many experimental situations: A detailed look at the concentration-response curves in Fig. 3 show that (-)-CM-TPMF and (-)-B-TPMF can be applied up to 200 nM (causing 90 % inhibition and 40 % enhancement of $K_{Ca}2.1$) without significant functional activity on the other subtypes. (A note of caution: Due to the $Ca^{2+}$-dependent modulatory actions of both compounds the corresponding percentages for natively expressed channels may deviate slightly). The reversibility properties of both compounds (Fig. 2) are also promising with respect to their use in a sequential manner on the same cell, at least in isolated neuronal preparations. We tentatively suggest that the opposite effects of (-)-CM-TPMF and (-)-B-TPMF on biological responses obtained from complex in vitro or in vivo biological systems - possibly combined with lack of effects of their respective

Molecular Pharmacology Fast Forward. Published on November 1, 2011 as DOI: 10.1124/mol.111.074252
This article has not been copyedited and formatted. The final version may differ from this version.



(+)-enantiomers - would be a strong indication of the participation of the $K_{Ca}2.1$ isoform in that particular process.

Molecular Pharmacology Fast Forward. Published on November 1, 2011 as DOI: 10.1124/mol.111.074252
This article has not been copyedited and formatted. The final version may differ from this version.



**Acknowledgements**

A very special thank you to Sofia Hammami for her dedicated and highly significant contribution to the electrophysiological work conducted during her four week sabbatical at NeuroSearch A/S in January 2011. The authors also greatly appreciate the expert technical assistance provided by Lene Gylle Larsen (molecular biology), Susanne Kalf Hansen, Anne Stryhn Meincke, Vibeke Meyland-Smith, and Jette Sonne (electrophysiology and cell culturing), as well as Torben Skov (determination of chiral purity) and Tove Thomsen (optical rotation measurements). Dr. Heike Wulff and Dr. Gordon Munro are acknowledged for critical reading of the manuscript.

Molecular Pharmacology Fast Forward. Published on November 1, 2011 as DOI: 10.1124/mol.111.074252
This article has not been copyedited and formatted. The final version may differ from this version.



**Authorship Contributions**

Participated in research design: Palle Christophersen, Charlotte Hougaard, Dorte Strøbæk, Marianne L. Jensen.

Conducted experiments: Charlotte Hougaard, Sofia Hammami.

Contributed new reagents or analytic tools: Birgitte L. Eriksen, Ulrik S. Sørensen, Marianne L. Jensen.

Performed data analysis: Charlotte Hougaard, Sofia Hammami.

Wrote or contributed to the writing of the manuscript: Palle Christophersen, Charlotte Hougaard, Dorte Strøbæk, Ulrik S. Sørensen, Marianne L. Jensen, Birgitte L. Eriksen.

Molecular Pharmacology Fast Forward. Published on November 1, 2011 as DOI: 10.1124/mol.111.074252
This article has not been copyedited and formatted. The final version may differ from this version.



## References

Alviña K and Khodakhah K (2010) $K_{Ca}$ channels as therapeutic targets in episodic ataxia type-2. *J Neurosci* **30:**7249-7257.

Armstrong WE, Rubrum A, Teruyama R, Bond CT, and Adelman JP (2005) Immunocytochemical localization of small-conductance, calcium-dependent potassium channels in astrocytes of the rat supraoptic nucleus. *J Comp Neurol* **491:**175-185.

Bond CT, Herson PS, Strassmaier T, Hammond R, Stackman R, Maylie J, and Adelman JP (2004) Small conductance $Ca^{2+}$-activated $K^+$ channel knock-out mice reveal the identity of calcium-dependent afterhyperpolarization currents. *J Neurosci* **24:**5301-5306.

Bond CT, Maylie J, and Adelman JP (2005) SK channels in excitability, pacemaking and synaptic integration. *Curr Opin Neurobiol* **15**:305-311

Bruening-Wright A, Lee WS, Adelman JP, and Maylie J (2007) Evidence for a deep pore activation gate in small conductance $Ca^{2+}$-activated $K^+$ channels. *J Gen Physiol* **130:**601-610.

Bruening-Wright A, Schumacher MA, Adelman JP, and Maylie J (2002) Localization of the activation gate for small conductance $Ca^{2+}$-activated $K^+$ channels. *J Neurosci* **22:**6499-6506.

Eriksen BL, Hougaard C, Strøbæk D, Christophersen P, and Sørensen US (2010a) Substituted [1,2,4]triazolo[1,5-a]pyrimidines and their use as potassium channel modulators. International Patent no. WO2010/112484.

Eriksen BL, Hougaard C, Strøbæk D, Christophersen P, and Sørensen US (2010b) Substituted [1,2,4]triazolo[1,5-a]pyrimidines and their use as potassium channel modulators. International Patent no. WO2010/112485.

Eriksen BL, Hougaard C, Strøbæk D, Christophersen P, and Sørensen US (2010c) Substituted [1,2,4]triazolo[1,5-a]pyrimidines and their use as potassium channel modulators. International Patent no. WO2010/112486

Galeotti N, Ghelardini C, Caldari B, and Bartolini A (1999) Effect of potassium channel modulators in mouse forced swimming test. *Br J Pharmacol* **126:**1653-1659.

Garneau L, Klein H, Banderali U, Longpré-Lauzon A, Parent L, and Sauvé R (2009) Hydrophobic interactions as key determinants to the KCa3.1 channel closed configuration. An analysis of KCa3.1 mutants constitutively active in zero $Ca^{2+}$. *J Biol Chem* **284:**389-403.

Greenberg DA, Cooper EC, and Carpenter CL (1984) Calcium channel 'agonist' BAY K 8644 inhibits calcium antagonist binding to brain and PC12 cell membranes. *Brain Res* **305:**365-368.

Hopf FW, Bowers MS, Chang SJ, Chen BT, Martin M, Seif T, Cho SL, Tye K, and Bonci A (2010) Reduced nucleus accumbens SK channel activity enhances alcohol seeking during abstinence. *Neuron* **65:**682-694.

Hopf FW, Simms JA, Chang SJ, Seif T, Bartlett SE, and Bonci A (2011) Chlorzoxazone, an SK-type potassium channel activator used in humans, reduces excessive alcohol intake in rats. *Biol Psychiatry* **69:**618-624.

Hougaard C, Eriksen BL, Jørgensen S, Johansen TH, Dyhring T, Madsen LS, Strøbæk D, and Christophersen P (2007) Selective positive modulation of the SK3 and SK2 subtypes of small conductance $Ca^{2+}$-activated $K^+$ channels. *Br J Pharmacol* **151:**655-665.

Hougaard C, Jensen ML, Dale TJ, Miller DD, Davies DJ, Eriksen BL, Strøbæk D, Trezise DJ, and Christophersen P (2009) Selective activation of the SK1 subtype of human small-

conductance $Ca^{2+}$-activated $K^+$ channels by 4-(2-methoxyphenylcarbamoyloxymethyl)-piperidine-1-carboxylic acid *tert*-butyl ester (GW542573X) is dependent on serine 293 in the S5 segment. *Mol Pharmacol* **76:**569-578.

Jacobsen JP, Weikop P, Hansen HH, Mikkelsen JD, Redrobe JP, Holst D, Bond CT, Adelman JP, Christophersen P, and Mirza NR (2008) SK3 $K^+$ channel-deficient mice have enhanced dopamine and serotonin release and altered emotional behaviors. *Genes Brain Behav* **7:**836-848.

Janahmadi M, Goudarzi I, Kaffashian MR, Behzadi G, Fathollahi Y, and Hajizadeh S (2009) Co-treatment with riluzole, a neuroprotective drug, ameliorates the 3-acetylpyridine-induced neurotoxicity in cerebellar Purkinje neurones of rats: behavioural and electrophysiological evidence. *Neurotoxicol* **30:**393-402.

Jenkins DP, Strøbæk D, Hougaard C, Jensen ML, Hummel R, Sørensen US, Christophersen P, and Wulff H (2011) Negative gating modulation by (*R*)-N-(Benzimidazol-2-yl)-tetrahydro-1-naphtylamine (NS8593) depends on residues in the inner pore vestibule: pharmacological evidence of deep-pore gating of $K_{Ca}2$ channels. *Mol Pharmacol* **79:**899-909.

Khanna R, Chang MC, Joiner WJ, Kaczmarek LK, and Schlichter LC (1999) hSK4/hIK1, a calmodulin-binding $K_{Ca}$ channel in human T lymphocytes. Roles in proliferation and volume regulation. *J Biol Chem* **274:**14838-14849.

Klein H, Garneau L, Banderali U, Simoes M, Parent L, and Sauvé R (2007) Structural determinants of the closed KCa3.1 channel pore in relation to channel gating: results from a substituted cysteine accessibility analysis. *J Gen Physiol* **129:**299-315.

Lamy C, Goodchild SJ, Weatherall KL, Jane DE, Liégeois JF, Seutin V, and Marrion NV (2010) Allosteric block of $K_{Ca}2$ channels by apamin. *J Biol Chem* **285:**27067-27077.

Li W and Aldrich RW (2011) Electrostatic influences of charged inner pore residues on the conductance and gating of small conductance $Ca^{2+}$ activated $K^+$ channels. *Proc Nat Acad Sci USA* **108:**5946-5953.

Li W, Halling DB, Hall AW, and Aldrich RW (2009) EF hands at the N-lobe of calmodulin are required for both SK channel gating and stable SK-calmodulin interaction. *J Gen Physiol* **134:**281-293.

Pedarzani P, Mosbacher J, Rivard A, Cingolani LA, Oliver D, Stocker M, Adelman JP, and Fakler B (2001) Control of electrical activity in central neurons by modulating the gating of small conductance $Ca^{2+}$-activated $K^+$ channels. *J Biol Chem* **276:**9762-9769.

Pedarzani P and Stocker M (2008) Molecular and cellular basis of small- and intermediate-conductance, calcium-activated potassium channel function in the brain. *Cell Mol Life Sci* **65:**3196-3217.

Rimini R, Rimland JM, and Terstappen GC (2000) Quantitative expression analysis of the small conductance calcium-activated potassium channels, SK1, SK2 and SK3, in human brain. *Mol Brain Res* **85:**218-220

Ristori G, Romano S, Visconti A, Cannoni S, Spadaro M, Frontali M, Pontieri FE, Vanacore N, and Salvetti M (2010) Riluzole in cerebellar ataxia: a randomized, double-blind, placebo-controlled pilot trial. *Neurology* **74:**839-845.

Sieghart W (1994) Pharmacology of benzodiazepine receptors: an update. *J Psyc Neurosci* **191:**24-29.

Sørensen US, Strøbæk D, Christophersen P, Hougaard C, Jensen ML, Nielsen EØ, Peters D, and Teuber L (2008) Synthesis and structure-activity relationship studies of 2-(N-substituted)-aminobenzimidazoles as potent negative gating modulators of small conductance $Ca^{2+}$-activated $K^+$ channels. *J Med Chem* **51:**7625-7634.

Strøbæk D, Hougaard C, Johansen TH, Sørensen US, Nielsen EØ, Nielsen KS, Taylor RD, Pedarzani P, and Christophersen P (2006) Inhibitory gating modulation of small conductance $Ca^{2+}$-activated $K^+$ channels by the synthetic compound (*R*)-N-(benzimidazol-2-yl)-1,2,3,4-tetrahydro-1-naphtylamine (NS8593) reduces afterhyperpolarizing current in hippocampal CA1 neurons. *Mol Pharmacol* **70:**1771-1782.

Terstappen GC, Pellacani A, Aldegheri L, Graziani F, Carignani C, Pula G, and Virginio C (2003) The antidepressant fluoxetine blocks the human small conductance calcium-activated potassium channels SK1, SK2 and SK3. *Neurosci Lett* **346:**85-88.

Walter JT, Alviña K, Womack MD, Chevez C, and Khodakhah K (2006) Decreases in the precision of Purkinje cell pacemaking cause cerebellar dysfunction and ataxia. *Nature* **9:**389-397.

Wulff H and Zhorov BS (2008) $K^+$ channel modulators for the treatment of neurological disorders and autoimmune diseases. *Chem Rev* **108:**1744-1773.

Xia XM, Fakler B, Rivard A, Wayman G, Johnson-Pais T, Keen JE, Ishii T, Hirschberg B, Bond CT, Lutsenko S, Maylie J, and Adelman JP (1998) Mechanism of calcium gating in small-conductance calcium-activated potassium channels. *Nature* **395:**503-507.

Molecular Pharmacology Fast Forward. Published on November 1, 2011 as DOI: 10.1124/mol.111.074252
This article has not been copyedited and formatted. The final version may differ from this version.



**Legends to Figures**

Fig. 1. Chemical structures of the negative $K_{Ca}2.1$ channel modulator B-TPMF and the positive modulators CM-TPMF and GW542573X.

Fig. 2. (-)-CM-TPMF acts as an activator and (-)-B-TPMF acts as an inhibitor of $K_{Ca}2.1$ channels. A, whole-cell current recorded from HEK293 cells stably expressing $K_{Ca}2.1$. I-V relationships were obtained at symmetrical $[K^+]$ and with the free $[Ca^{2+}]$ in the pipette solution buffered to 0.3 μM. I-V relationships were measured upon application of 200-ms voltage ramps (-80 to +80 mV), elicited every 5 s from a holding potential of 0 mV in the absence (Ctrl) or in the presence of 10 nM of the compounds, (+)-B-TPMF, (-)-B-TPMF, (+)-CM-TPMF and (-)-CM-TPMF, as indicated. B, whole-cell $K_{Ca}2.1$ current at -75 mV obtained from the voltage ramps (A) as a function of time. The cell was exposed to 10 nM of the (-)- and (+)-forms of CM-TPMF and B-TPMF as indicated by the bars. C, average currents (mean ± S.E.M.) in the presence of (-)- and (+)-forms of CM-TPMF and B-TPMF (10 nM). Current measured in the presence of compound is shown relative to the current level prior to compound addition (control; n = 4 – 11). (-)-B-TPMF was more potent than (+)-B-TPMF ($p < 0.001$, students t-test) in inhibiting $K_{Ca}2.1$ current, while (-)-CM-TPMF was more potent than (+)-CM-TPMF in potentiating the current ($p < 0.001$, students t-test).

Fig. 3. (-)-B-TPMF is a $K_{Ca}2.1$ subtype selective inhibitor and (-)-CM-TPMF a $K_{Ca}2.1$ selective activator. A, I-V relationships measured from inside-out patches obtained from HEK293 cells stably expressing $hK_{Ca}2.1$, $hK_{Ca}2.2$ or $hK_{Ca}2.3$. Each I-V plot shows a control trace, a trace obtained in the presence of 30 nM (-)-B-TPMF and a trace in the presence of 30 nM (-)-CM-

Molecular Pharmacology Fast Forward. Published on November 1, 2011 as DOI: 10.1124/mol.111.074252
This article has not been copyedited and formatted. The final version may differ from this version.



TPMF. The free [$Ca^{2+}$] in the bath/intracellular solution was 0.3 μM (resulting in approximately 30% of the maximal current level) to allow for both positive and negative modulation. B, concentration-response relationships of (-)-B-TPMF on the three $K_{Ca}2$ subtypes. Residual current is depicted as a function of the (-)-B-TPMF concentration. Currents were measured from inside-out patches at 0.5 μM free $Ca^{2+}$ (approximately 90% of the maximal current level) and each data point is the mean ± S.E.M. of 5-7 experiments. The solid lines are the fit of data to the Hill equation yielding the following $IC_{50}$ values and Hill coefficients: $K_{Ca}2.1$: 0.031 μM and -1.2; $K_{Ca}2.2$: 1.05 μM and -1.7; $K_{Ca}2.3$: 1.32 μM and -1.7. C, concentration-response relationships of (-)-CM-TPMF on $K_{Ca}2.1$, $K_{Ca}2.2$ and $K_{Ca}2.3$. Currents were measured from inside-out patches at 0.2 μM free $Ca^{2+}$ (approximately 15% activation) and shown relative to the current level obtained at 10 μM $Ca^{2+}$ in the absence of compound. Each data point is the mean ± S.E.M. of 6-8 experiments and the solid lines are the fit of data to the Hill equation yielding the following $EC_{50}$ values and Hill coefficients $K_{Ca}2.1$: 0.024 μM and 0.8; $K_{Ca}2.2$: 0.29 μM and 1.5; $K_{Ca}2,3$: 0.25 μM and 1.1. Efficacy with respect to saturating $Ca^{2+}$ was in the range 83-87%.

Fig. 4. (-)-CM-TPMF is a $K_{Ca}2$ channel opener and a positive modulator. A, $K_{Ca}2.1$ current at -75 mV, measured from an inside-out patch and depicted as a function of time. The patch was exposed to 0.1 μM (-)-CM-TPMF either in the absence of $Ca^{2+}$ (0), at 0.2 – or at 10 μM $Ca^{2+}$. B, I-V relationships at 0, 0.2 - or 10 μM $Ca^{2+}$ in the absence (Ctrl) or presence of 0.1 μM (-)-CM-TPMF as indicated. C, $Ca^{2+}$-response curves for $K_{Ca}2.1$ measured from inside-out patches either in the absence (Ctrl) or in the presence of (-)-CM-TPMF (0.1 μM or 1 μM). Currents from individual patches were normalized with respect to the effect of 10 μM $Ca^{2+}$. Data points are the mean ± S.E.M. of at least 6 experiments. The lines are the fit of data to the Hill equation yielding

Molecular Pharmacology Fast Forward. Published on November 1, 2011 as DOI: 10.1124/mol.111.074252
This article has not been copyedited and formatted. The final version may differ from this version.



the following $EC_{50}$ values and Hill coefficients: Ctrl: 0.32 µM and 4.4, 0.1 µM (-)-CM-TPMF: 0.15 µM and 2.9, 1 µM (-)-CM-TPMF: 0.13 µM and 2.8. Note the substantial $Ca^{2+}$-independent opener effect of (-)-CM-TPMF at very low $Ca^{2+}$ concentrations (14 ± 3% and 32 ± 5% of maximal activity at 0.1 µM and 1 µM (-)-CM-TPMF) and the higher efficacy at saturating $Ca^{2+}$ (I/Imax > 1) in the presence of (-)-CM-TPMF.

Fig. 5. (-)-B-TPMF inhibits the $K_{Ca}2.1$ current in a $Ca^{2+}$-dependent manner. A, $K_{Ca}2.1$ current at -75 mV plotted versus time. Current was measured from an inside-out patch exposed to 30 nM (-)-B-TPMF either at 0.3 or 10 µM $Ca^{2+}$. As control for the background/leak current level, periods with 0 free $Ca^{2+}$ were included. B, % current inhibition induced by (-)-B-TPMF (30 nM) at the different $Ca^{2+}$ concentrations. Data points are the mean ± S.E.M. of 5-6 experiments at each $Ca^{2+}$ concentration.

Fig. 6. Maximal (-)-CM-TPMF activation concentration-dependently decreases the apparent affinity of the inhibitor (-)-B.TPMF. A, I-V relationships measured from inside-out patches obtained from HEK293 cells stably expressing $hK_{Ca}2.1$ at a free [$Ca^{2+}$] of 0.2 µM. I-V curves were obtained in the presence of 1 or 10 µM (-)-CM-TPMF alone or in combination with 1 µM (-)-B-TPMF. B, concentration-response relationship of (-)-B-TPMF in the presence of 1 or 10 µM (-)-CM-TPMF. Residual current is depicted as a function of the (-)-B-TPMF concentration. Each data point is the mean ± S.E.M. of 4-9 experiments and the solid lines are the fit of data to the Hill equation resulting in the following $IC_{50}$ values and Hill coefficients: 0.43 µM and -0.9 (at 1 µM (-)-CM-TPMF) and 2.96 µM and -1.4 (in the presence of 10 µM (-)-CM-TPMF).

Molecular Pharmacology Fast Forward. Published on November 1, 2011 as DOI: 10.1124/mol.111.074252
This article has not been copyedited and formatted. The final version may differ from this version.



Fig. 7. The reduced apparent affinity of (-)-B-TPMF is due to (-)-CM-TPMF competition, not the degree of channel activation. A, $K_{Ca}2.1$ current measured at -75 mV as a function of time. The inside of the patch was exposed to a [$Ca^{2+}$] of 0, 0.5 or 10 µM as indicated. (-)-B-TPMF was added once steady current activation was obtained by 10 µM $Ca^{2+}$ alone or by the combination of 0.5 µM $Ca^{2+}$ and 3 µM (-)-CM-TPMF. B, I-V relationships measured at the time points indicated by letters in A. Data is from a single experiment representative of 4 independent experiments.

Fig. 8. The activity of (-)-B-TPMF and (-)-CM-TPMF is critically dependent on Ser293 in $K_{Ca}2.1$. A, Schematic illustrating the approximate S5 location of the single amino acid that is mutated in the channel constructs. In $K_{Ca}2.1$, serine is replaced with leucine, which is the equivalent amino acid in $K_{Ca}2.3$, and in $K_{Ca}2.3$ leucine is replaced with serine. Amino acid alignment of the S5 region of $K_{Ca}2.1$ and $K_{Ca}2.3$ is shown on the right. B and C, I-V relationships measured from inside-out patches obtained from HEK293 cells transiently transfected with $K_{Ca}2.1_{S293L}$ (B) or $K_{Ca}2.3_{L476S}$ (C). Each plot shows a trace in the absence of compound (Ctrl), a trace in the presence of 30 nM (-)-B-TPMF and one in the presence of 30 nM (-)-CM-TPMF. The free [$Ca^{2+}$] in the bath/intracellular solution was 0.3 µM to allow for both positive and negative modulation of the current level. D, concentration-response relationship of (-)-B-TPMF on $K_{Ca}2.1_{S293L}$ and $K_{Ca}2.3_{L476S}$. Residual current in the presence of (-)-B-TPMF is depicted as a function of the (-)-B-TPMF concentration. Currents were measured from inside-out patches at 0.5 µM free $Ca^{2+}$ and each data point is the mean ± S.E.M. of 5-6 experiments. The solid lines are the fit of data to the Hill equation yielding the following $IC_{50}$ values and Hill coefficients: h$K_{Ca}2.1_{S293L}$: 0.81 µM and -1.2, $K_{Ca}2.3_{L476S}$: 0.05 µM and -1.6. For illustrative purposes, data obtained on wild type $K_{Ca}2.1$ and $K_{Ca}2.3$ is included as dotted lines. E,

Molecular Pharmacology Fast Forward. Published on November 1, 2011 as DOI: 10.1124/mol.111.074252
This article has not been copyedited and formatted. The final version may differ from this version.



concentration-response relationship of (-)-CM-TPMF on $K_{Ca}2.1_{S293L}$ and $K_{Ca}2.3_{L476S}$. Currents were measured at 0.2 µM free $Ca^{2+}$ and depicted relative to the current level obtained at 10 µM $Ca^{2+}$ and in the absence of compound. Data points are the mean ± S.E.M. of 4-5 experiments and the solid lines are the fit of data to the Hill equation: $hK_{Ca}2.1_{S293L}$: 0.7 µM and 1.3, $K_{Ca}2.3_{L476S}$: 0.03 µM and 1.2. Efficacy with respect to maximal $Ca^{2+}$ was 89% ($hK_{Ca}2.1_{S293L}$) and 85% ($K_{Ca}2.3_{L476S}$). Again, for illustrative purposes, data on $K_{Ca}2.1$ and $K_{Ca}2.3$ are included as dotted lines.

**Table 1** Effects of CM-TPMF and B-TPMF at various ion channels

| [a] at 0.2 µM $[Ca^{2+}]_i$<br>[b] at 0.5 µM $[Ca^{2+}]_i$ | | (-)-CM-TPMF | | (+)-CM-TPMF | (-)-B-TPMF | | (+)-B-TPMF |
|---|---|---|---|---|---|---|---|
| | | $EC_{50}$ (µM)[a] | Hill slope | | $IC_{50}$ (µM)[b] | Hill slope | |
| **Inside-out** | $hK_{Ca}2.1$ | 0.024 | 0.8 | | 0.031 | -1.2 | |
| | $hK_{Ca}2.2$ | 0.29 | 1.5 | | 1.05 | -1.7 | |
| | $hK_{Ca}2.3$ | 0.25 | 1.1 | | 1.32 | -1.7 | |
| | $hK_{Ca}2.3_{L476S}$ | 0.03 | 1.2 | | 0.05 | -1.6 | |
| **Whole cell** | | $SC_{100}$ in µM (n) | | $SC_{100}$ in µM (n) | $K_d$ in µM (n) | | $K_d$ in µM (n) |
| | $hK_{Ca}2.1$ | 0.0053 ± 0.00021 (6) | | 0.19 ± 0.044 (5) | 0.015 ± 0.0067 (5) | | 1.6 ± 0.54 (5) |
| | $hK_{Ca}2.2$ | 0.17 ± 0.05 (4) | | 2.6 ± 0.50 (4) | 0.29 ± 0.039 (4) | | 13 ± 3.2(4) |
| | $hK_{Ca}2.3$ | 0.047 ± 0.0049 (6) | | 1.5 ± 0.07 (4) | 0.23 ± 0.05 (4) | | 10 ± 2.3 (8) |
| | $hK_{Ca}3.1$ | 0.12 ± 0.0049 (5) | | 2.1 ± 0.12 (4) | $SC_{100}$ = 5.2 ± 1.0 µM (6) | | 35 ± 3.5 (3) |
| | | % inhibition at 10 µM (n) | | | % inhibition at 10 µM (n) | | |
| | $hK_{Ca}1.1$ | 39 ± 3.0 (3) | | | 20 ± 5.2 (3) | | |
| | $hK_v7.2+7.3$ | 1.3 ± 1.3 (4) | | | 12 ± 2.5 (4) | | |
| | $hK_v11.1$ | 37 ± 3.9 (3) | | | 36 ± 4.0 (3) | | |
| | $rNa_v1.2$ | 8.3 ± 2.8 (4) | | | 26 ± 3.1 (3) | | |

Compiled effects of (-) and (+) enantiomers of both CM-TPMF and B-TPMF on different cloned ion channels and constructs. Different potency/effect measures ($EC_{50}$, $IC_{50}$, $K_d$, $SC_{100}$, and % inhibition) have been applied as explained in Materials and Methods. [a] and [b] denotes the calculated free $Ca^{2+}$-concentrations used in the inside-out experiments. The h and r prefixes mean human and rat. The values are means ± S.E.M, n is the number of independent experiments.

# Figure 1

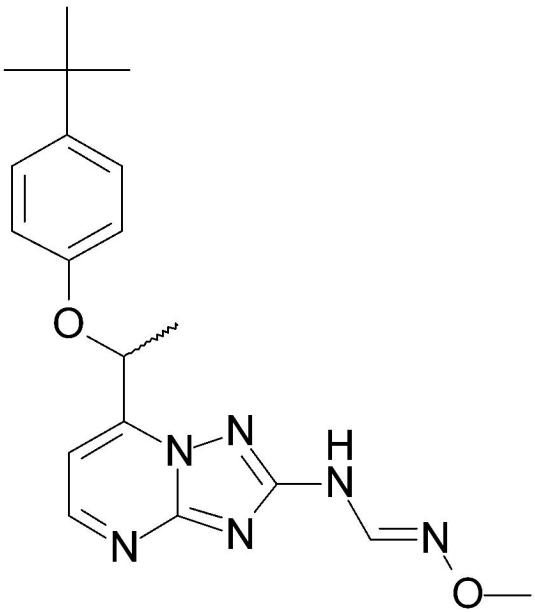

B-TPMF
*inhibitor*

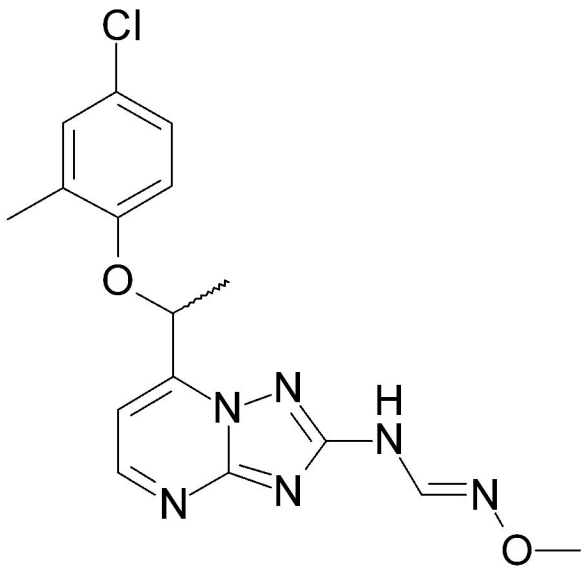

CM-TPMF
*activator*

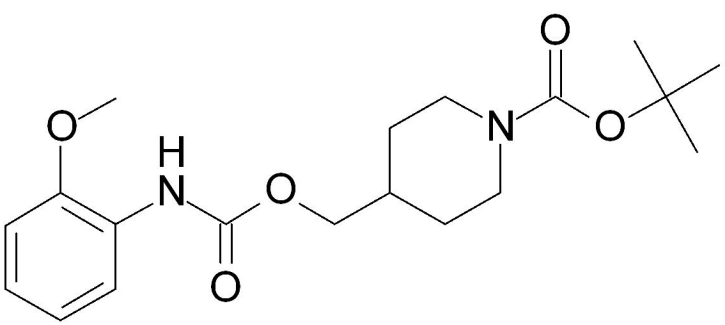

GW542573X
*activator*

# Figure 2

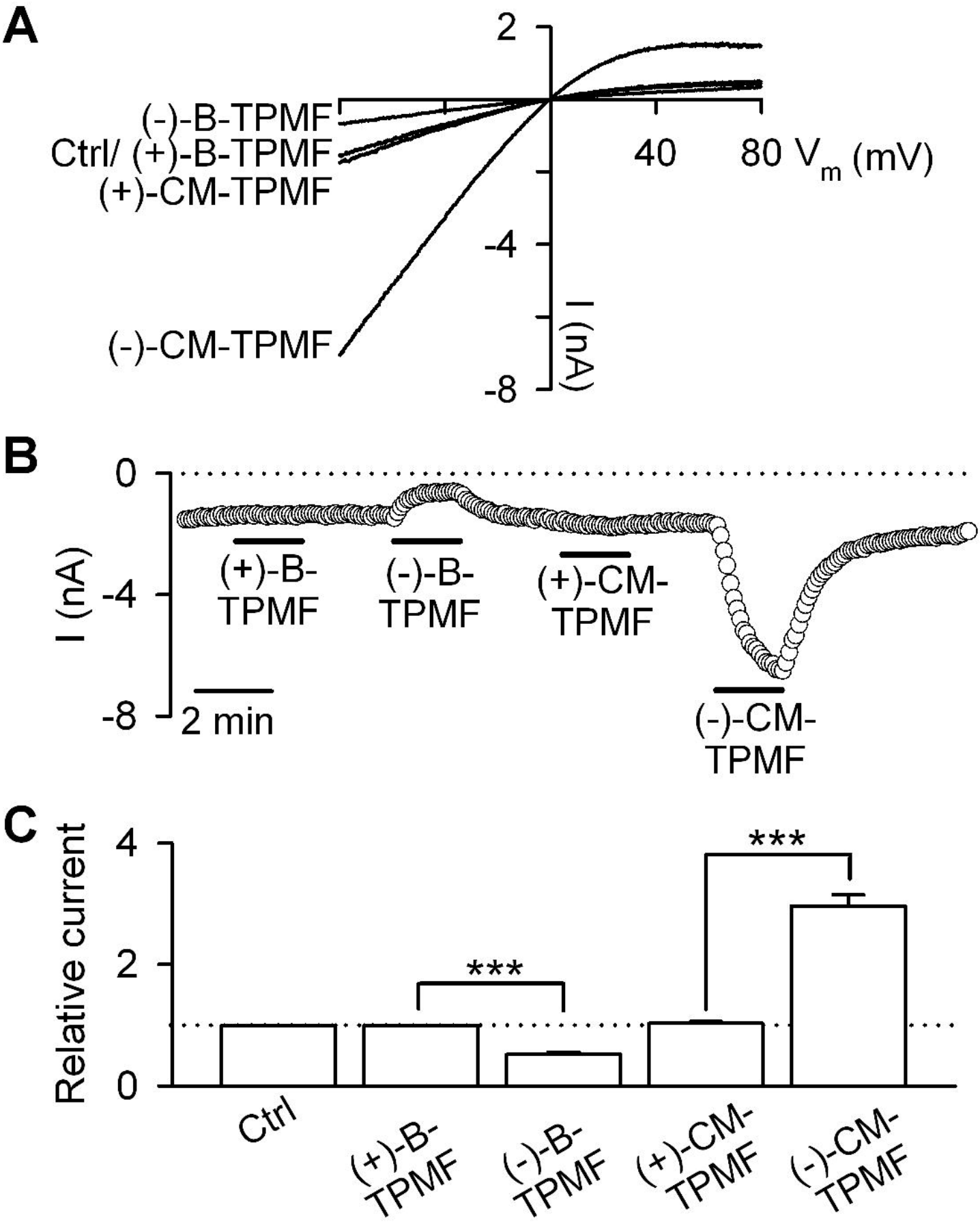
A
2
(-)-B-TPMF
Ctrl/ (+)-B-TPMF
(+)-CM-TPMF
40
80 V_m (mV)
-4
(-)-CM-TPMF
I (nA)
-8
B
0
I (nA)
-4
-8
(+)-B-TPMF
(-)-B-TPMF
(+)-CM-TPMF
2 min
(-)-CM-TPMF
C
Relative current
4
2
0
***
***
Ctrl
(+)-B-TPMF
(-)-B-TPMF
(+)-CM-TPMF
(-)-CM-TPMF

# Figure 3

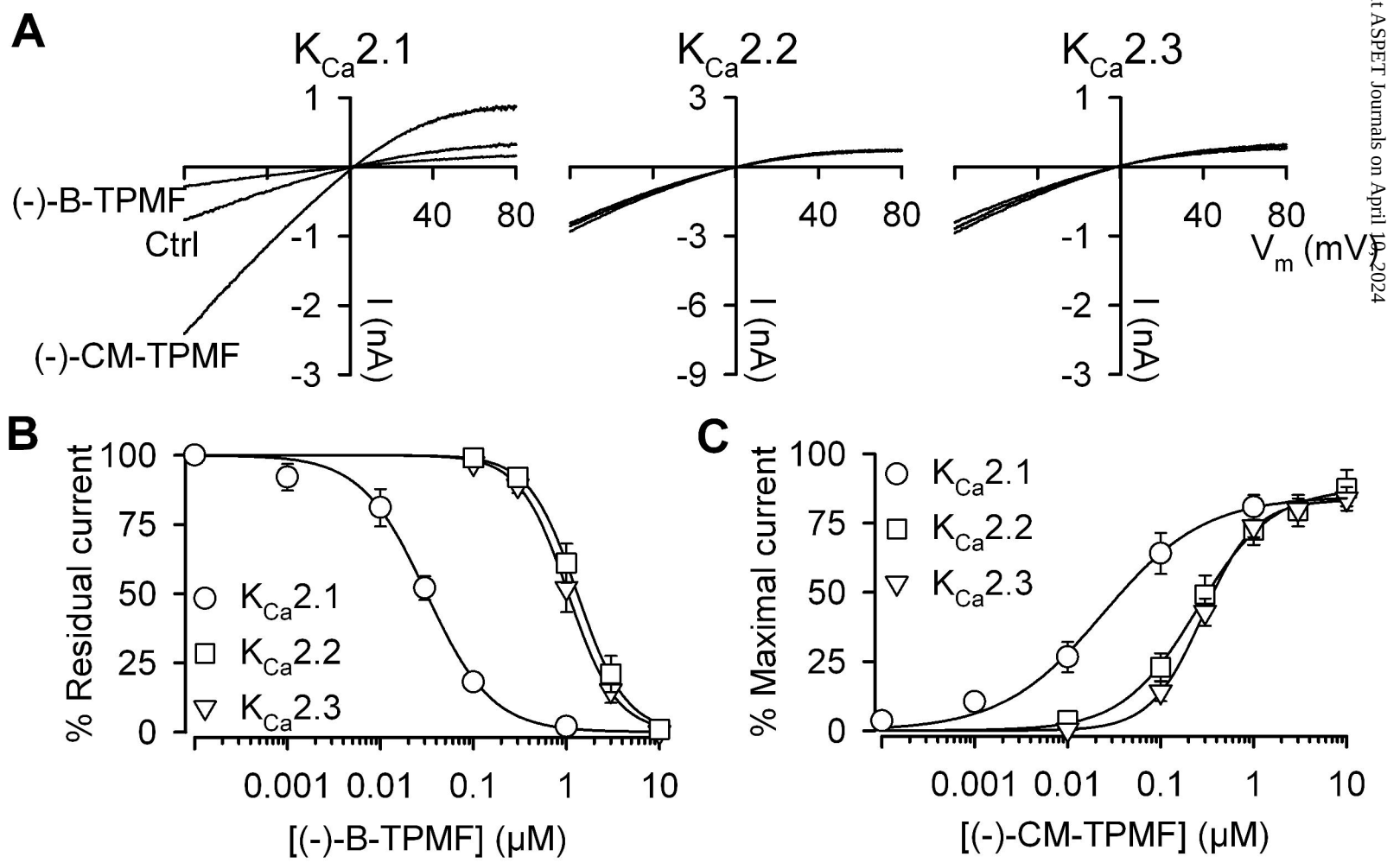

# Figure 4

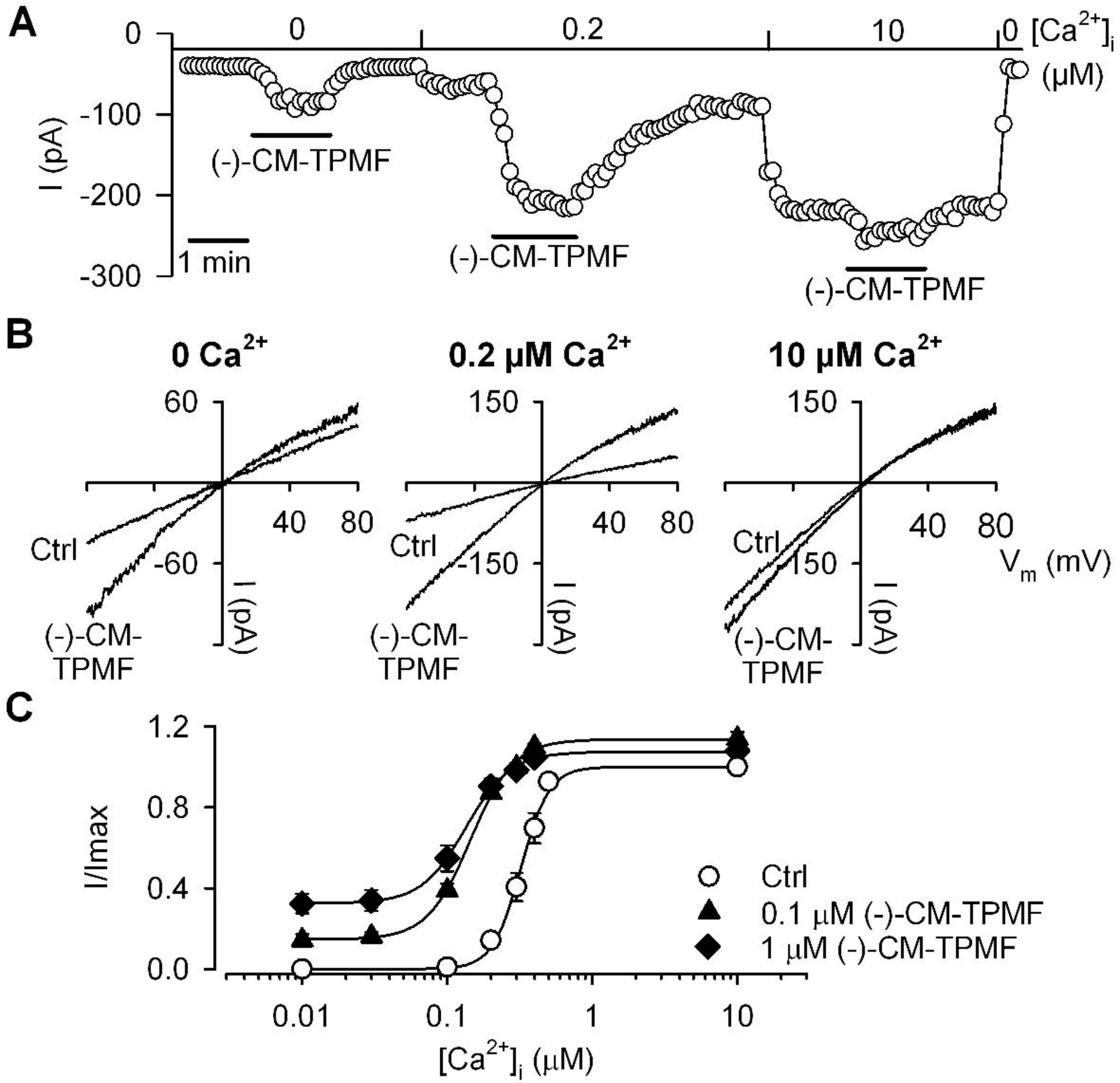
A
0
0
0.2
10
0 [Ca2+]i
(μM)
I (pA)
-100
-200
-300
(-)-CM-TPMF
1 min
(-)-CM-TPMF
(-)-CM-TPMF
B
0 Ca2+
0.2 μM Ca2+
10 μM Ca2+
60
150
150
40
80
40
80
40
80
Ctrl
-60
Ctrl
-150
Ctrl
150
Vm (mV)
I (pA)
I (pA)
I (pA)
(-)-CM-TPMF
(-)-CM-TPMF
(-)-CM-TPMF
C
1.2
0.8
0.4
0.0
I/Imax
Ctrl
0.1 μM (-)-CM-TPMF
1 μM (-)-CM-TPMF
0.01
0.1
1
10
[Ca2+]i (μM)

# Figure 5

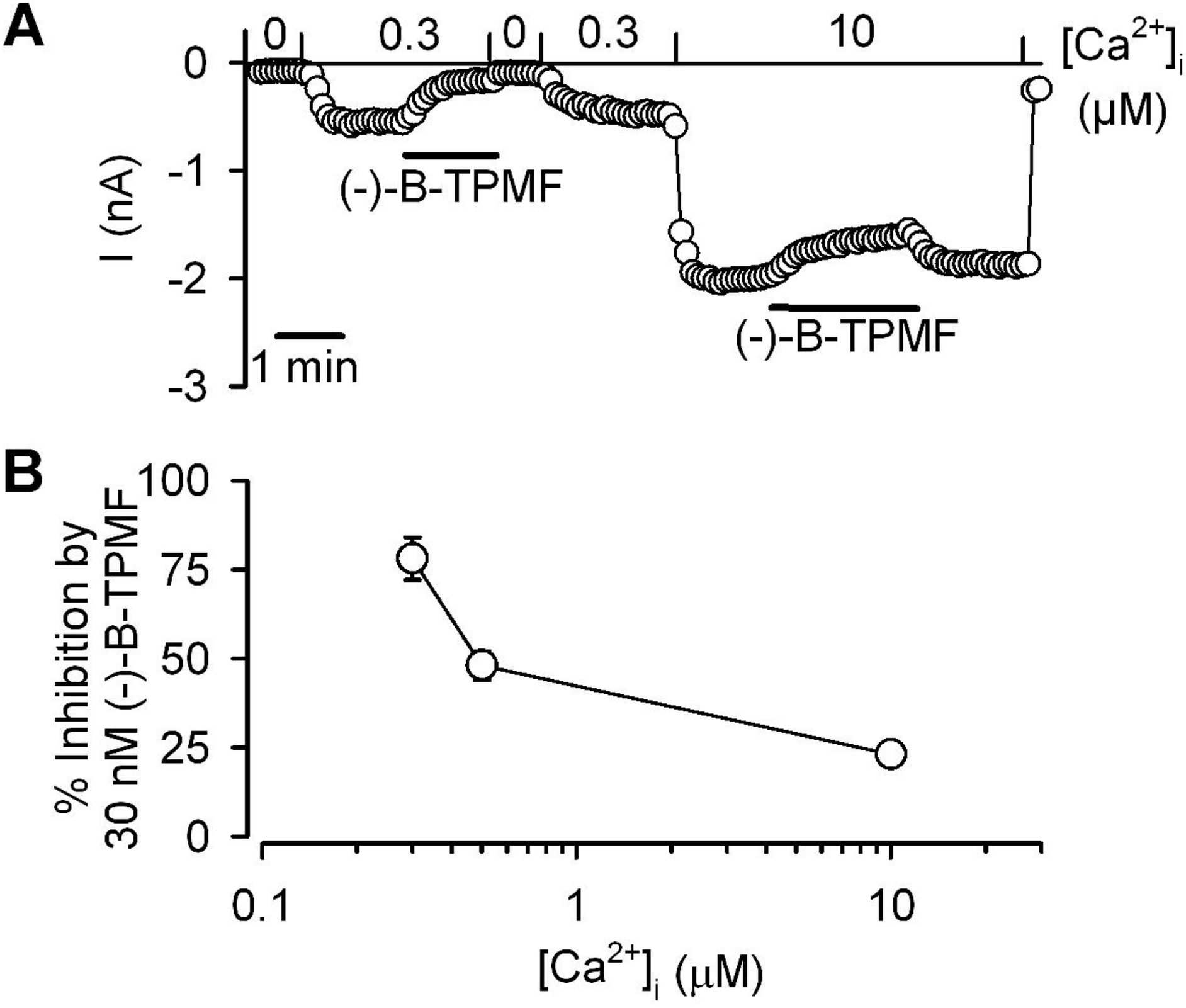
A
0
0.3
0
0.3
10
[Ca2+]i
(μM)
0
-1
-2
-3
I (nA)
(-)-B-TPMF
(-)-B-TPMF
1 min
B
% Inhibition by
30 nM (-)-B-TPMF
100
75
50
25
0
0.1
1
10
[Ca2+]i (μM)

# Figure 6

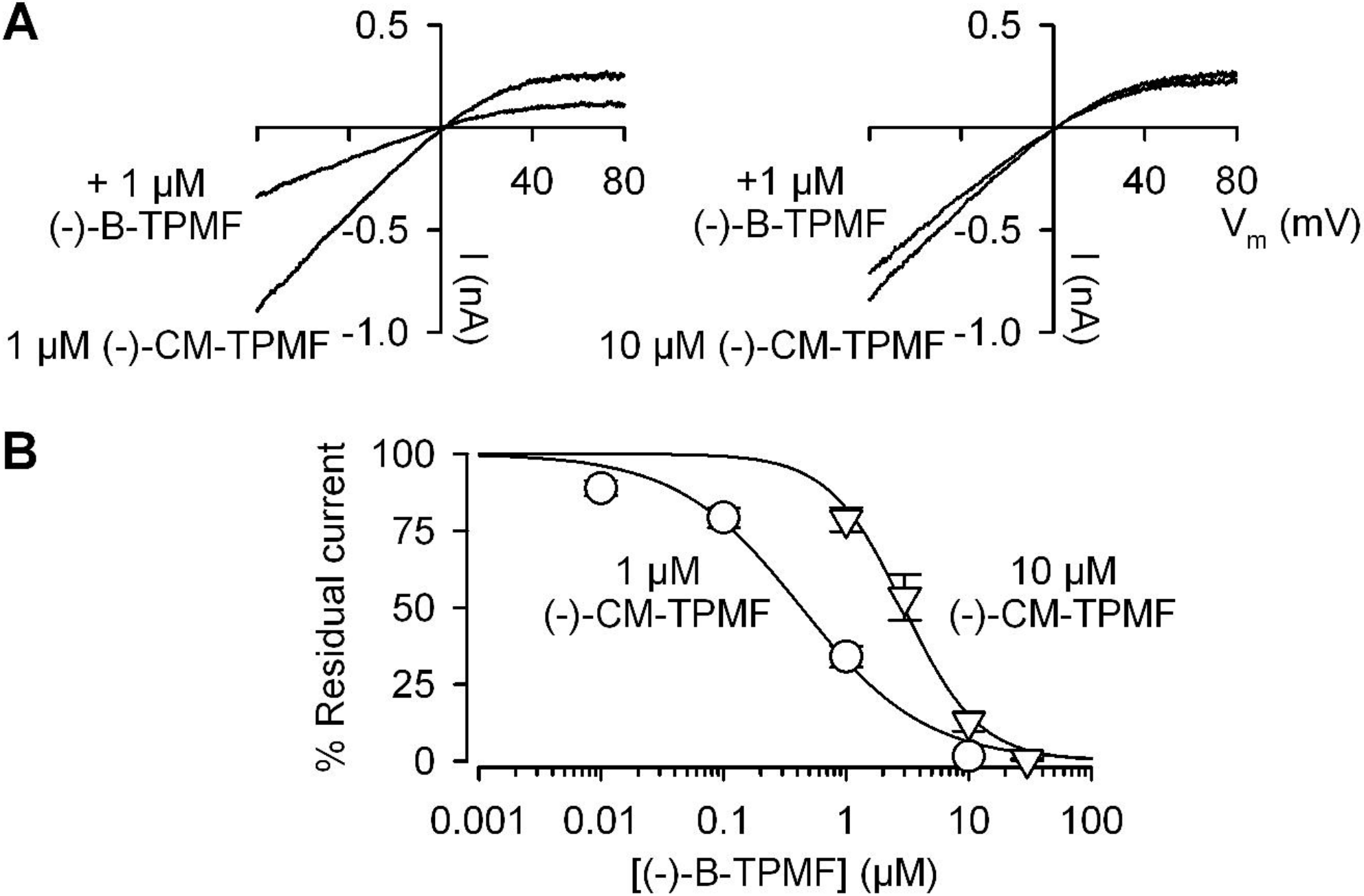
A
0.5
40
80
+ 1 µM
(-)-B-TPMF
-0.5
I (nA)
1 µM (-)-CM-TPMF
-1.0
0.5
40
80
+1 µM
(-)-B-TPMF
-0.5
V_m (mV)
I (nA)
10 µM (-)-CM-TPMF
-1.0
B
% Residual current
100
75
50
25
0
1 µM
(-)-CM-TPMF
10 µM
(-)-CM-TPMF
0.001
0.01
0.1
1
10
100
[(-)-B-TPMF] (µM)

# Figure 7

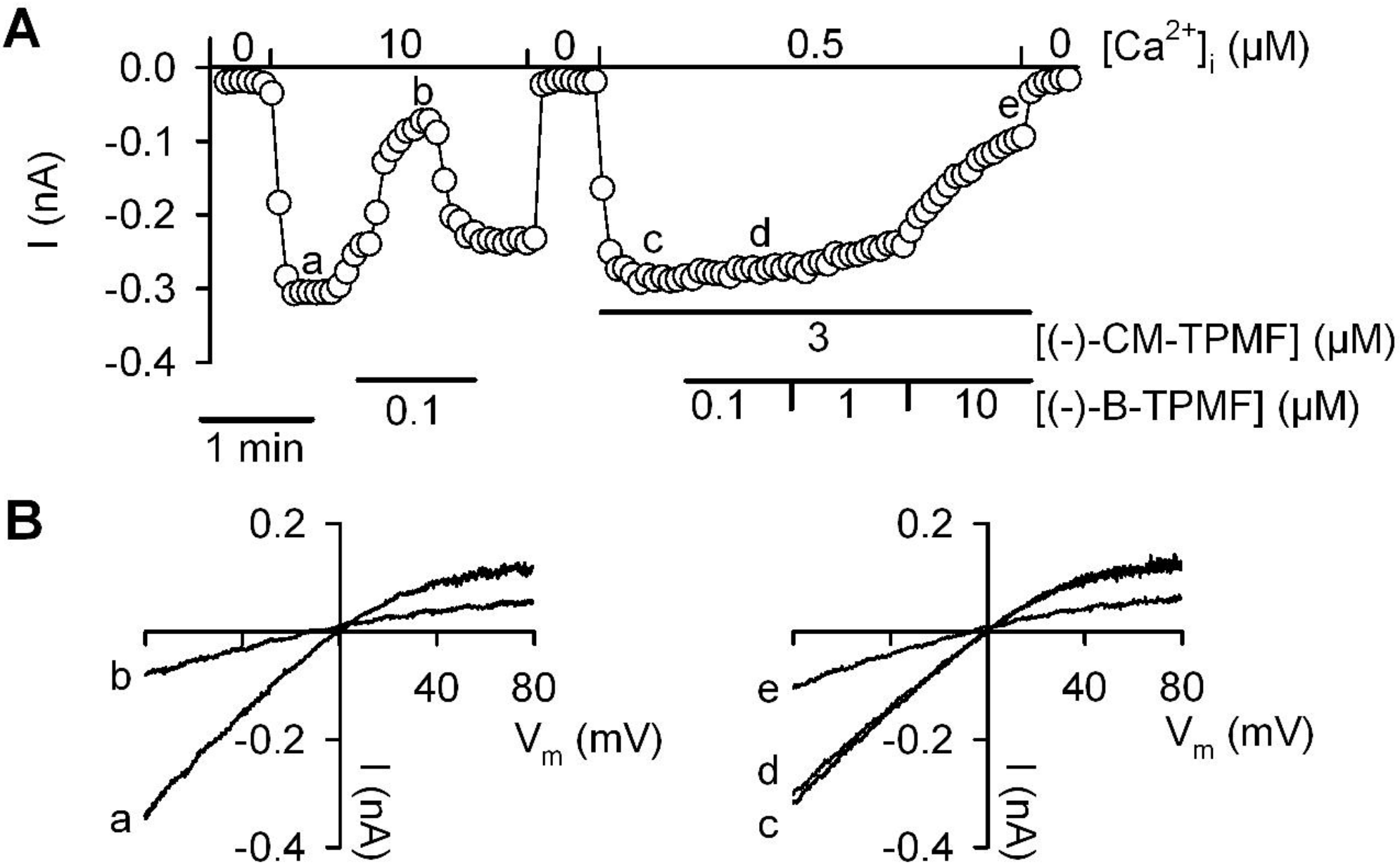
A
0
10
0
0.5
0
[Ca2+]i (μM)
0.0
-0.1
-0.2
-0.3
-0.4
I (nA)
a
b
c
d
e
3
[(-)-CM-TPMF] (μM)
0.1
0.1
1
10
[(-)-B-TPMF] (μM)
1 min
B
0.2
-0.2
-0.4
40
80
Vm (mV)
I (nA)
b
a
e
d
c

# Figure 8

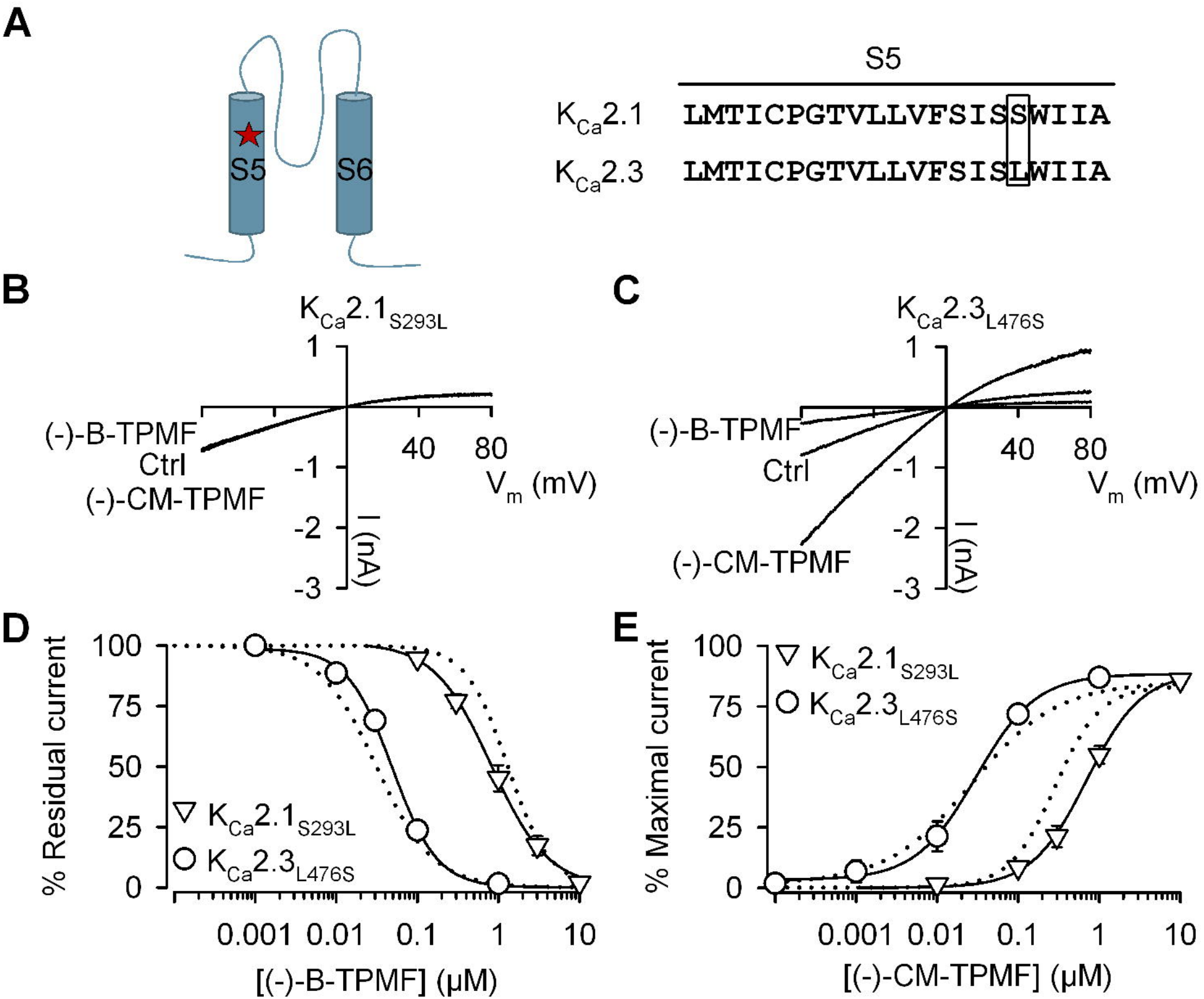
A
S5
S6
S5
$K_{Ca}2.1$ LMTICPGTVLLVFSISSWIIA
$K_{Ca}2.3$ LMTICPGTVLLVFSISLWIIA
B
$K_{Ca}2.1_{S293L}$
(-)-B-TPMF
Ctrl
(-)-CM-TPMF
1
-1
-2
-3
40
80
$V_m$ (mV)
I (nA)
C
$K_{Ca}2.3_{L476S}$
(-)-B-TPMF
Ctrl
(-)-CM-TPMF
1
-1
-2
-3
40
80
$V_m$ (mV)
I (nA)
D
% Residual current
100
75
50
25
0
$K_{Ca}2.1_{S293L}$
$K_{Ca}2.3_{L476S}$
0.001 0.01 0.1 1 10
[(-)-B-TPMF] (μM)
E
% Maximal current
100
75
50
25
0
$K_{Ca}2.1_{S293L}$
$K_{Ca}2.3_{L476S}$
0.001 0.01 0.1 1 10
[(-)-CM-TPMF] (μM)